Macromolecular Rapid Communications
www.mrc-journal.de

# Dynamic Contributions to the Bulk Mechanical Properties of Self-Assembled Polymer Networks with Reconfigurable Bonds

*Xiaomin Tang, Bingqing Wang, Sophia Eristoff, Han Zhang, and Christopher J. Bettinger**

**Soft materials that contain dynamic and reversible bonds exhibit unique properties including unusual extensibility, reversible elasticity, and self-healing capabilities, for example. Catechol motifs are of particular interest owing to their ability to form many kinds of reversible bonds; however, there are few reports on the role of hydrogen bonds between catechols. Here, physically crosslinked self-assembled networks composed of catechol-functionalized ABA triblock co-polymers are synthesized and characterized to elucidate the role of intermolecular bonding between catechol motifs on bulk mechanical properties. The Young's moduli of equilibrated networks range from 16 to 43 MPa. Furthermore, the concentration of intermolecular interaction is controlled indirectly by synthesizing polymers with prescribed catechol concentrations on each A block. Further, network dynamics are characterized by measuring the relaxation spectrum, and it is found that the network mean relaxation time is inversely related to catechol density. Finally, networks exhibit time-dependent recovery after uniaxial strain. These findings establish important relationships between molecular design, network composition, and macroscopic mechanical properties of model soft matter networks with dynamic intermolecular bonds. Furthermore, this insight has the potential to guide the design of dissipative materials for use in applications ranging from consumer products to surgical materials.**

Polymer networks that contain dynamic reversible bonds exhibit unusual properties such as extraordinary toughness,[1–3] self-healing capabilities,[4,5] and time dependent reversible elasticity.[6] These networks typically use reversible interactions such as metal–ligand coordination bonds,[6–8] hydrogen bonds,[9–11] ionic bonds,[3,12] and hydrophobic interactions.[13,14] Catechol motifs are of particular interest owing to their ability to form many types of reversible bonds.[15–19] Polymer networks with catechol–cation coordination bonds have relaxation times that are governed by the affinity of the cation with the catechol group.[20–22] Grindy et al.[23] measured the viscoelastic modulus for networks with kinetically distinct metal coordinate crosslinks and demonstrated that reversible coordination junctions dominate the viscoelasticity of bulk materials. Catechol motifs with two hydroxy groups can also form hydrogen bonds among themselves.[24] Comparatively, there have been few reports on the role of hydrogen bonds between catechols in crosslinked networks.[25] Furthermore, the role of catechol concentration on bulk mechanics of polymer networks has yet to be elucidated in networks composed of model polymers. Here, we describe the role of hydrogen-bonded catechols on the bulk mechanical properties of the resulting networks.

We recently synthesized catechol-bearing ABA triblock copolymers that can self-assemble into mechanically robust networks wherein physical crosslinks are stabilized by inter-chain hydrogen bonding.[26] The copolymer is synthesized through three steps and is processed into a network as shown in **Scheme 1**. Poly(ethylene glycol)-bromide (PEG-Br) macroinitiators are first prepared and then extended with an active esterified methacrylic acid (*N*-hydroxysuccinimide ester; NHSMA) by atom transfer radical polymerization. A blocks are then conjugated with dopamine to produce poly(NHSMA)$_{60}$-*b*-PEG$_{227}$-*b*-poly(NHSMA)$_{60}$-Cat (ABA-Cat) polymers with a targeted conjugation ratio ($r_{cat}$) defined as the fraction of NHSMA monomers functionalized with a pendant catechol. Solutions of ABA-Cat polymer in *N,N*-dimethylformamide (DMF) self-assemble into networks through solvent exchange with water. We posit the network contains physical crosslinks composed of catechol-rich A blocks bridged together by PEG-based B blocks for following reasons. First, A and B blocks are immiscible in water and will be phase separated. Our previous study on structure showed solvent exchange disrupts crystalized PEG block by differential scanning calorimetry[26] and hydrogen-bonded

Dr. X. Tang, B. Wang, S. Eristoff, Dr. C. J. Bettinger
Department of Materials Science and Engineering
Carnegie Mellon University
Pittsburgh, PA 15213, USA
E-mail: cbetting@andrew.cmu.edu
H. Zhang, Dr. C. J. Bettinger
Department of Biomedical Engineering
Carnegie Mellon University
Pittsburgh, PA 15213, USA
The ORCID identification number(s) for the author(s) of this article can be found under https://doi.org/10.1002/marc.201900551.

**DOI: 10.1002/marc.201900551**

 

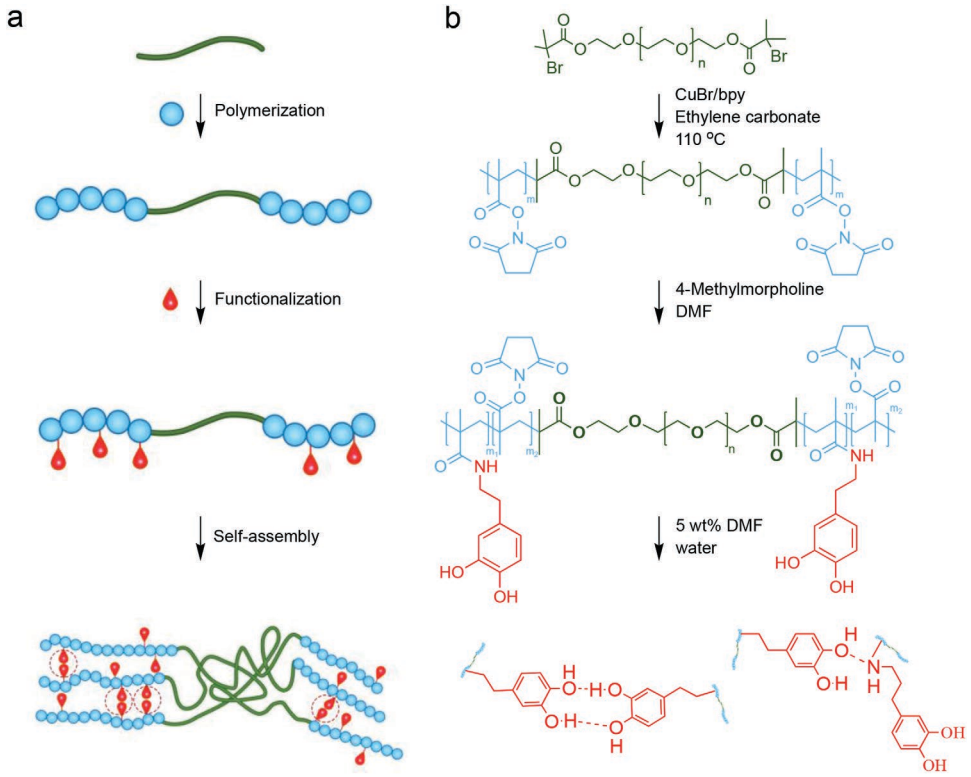


**Scheme 1.** Schematic showing a) the molecular structure and b) the corresponding chemical structures of the synthesis of poly(NHSMA)-*b*-PEG-*b*-poly(NHSMA)-Cat (ABA-Cat) triblock copolymers and the polymer processing to create hydrated ABA-Cat film.

catechols are confirmed by broad stretches in FTIR spectra from wavenumbers 3700 to 3100 $cm^{-1}$ (**Figure 1**a). In addition, previous work with similar structure system has shown microphase separation.[27–29] This model network is ideal for a systematic study of the role of hydrogen bonding on polymer dynamics for several reasons. First, the concentration of catechols in physical crosslinks enriched in A blocks can be precisely defined by controlling $r_{cat}$. Second, PEG B blocks have a known Chi parameter with water and a uniform molecular weight between crosslinks ($M_c$).

Amine reactive monomers in A blocks can achieve a conjugation ratio of $r_{cat}$ from 0 to 60% as calculated by $^1$H NMR (Figure S1, Supporting Information). Polymers with catechol conjugation ratios of $r_{cat}$ = 16 ± 4%, 38 ± 2%, and 61 ± 2.3% were used in subsequent experiments and are denoted as $r_{cat\text{-}16}$, $r_{cat\text{-}38}$, and $r_{cat\text{-}61}$, respectively. Less than 10% of −OH groups in networks prepared from $r_{cat\text{-}16}$, $r_{cat\text{-}38}$, and $r_{cat\text{-}61}$ polymers are free, which suggests strong coupling between catechols as measured by IR (Figure 1b). The overall concentration of catechols in self-assembled networks ($C_{cat\text{-}net}$) can be controlled indirectly by choosing $r_{cat}$ while the polymer volume fraction ($\phi_{2,s}$) is largely constant. Values for $C_{cat\text{-}net}$ were determined by gravimetry (see Supporting Information). As shown in Figure 1c, $C_{cat\text{-}net}$ can be tuned by varying $r_{cat}$.

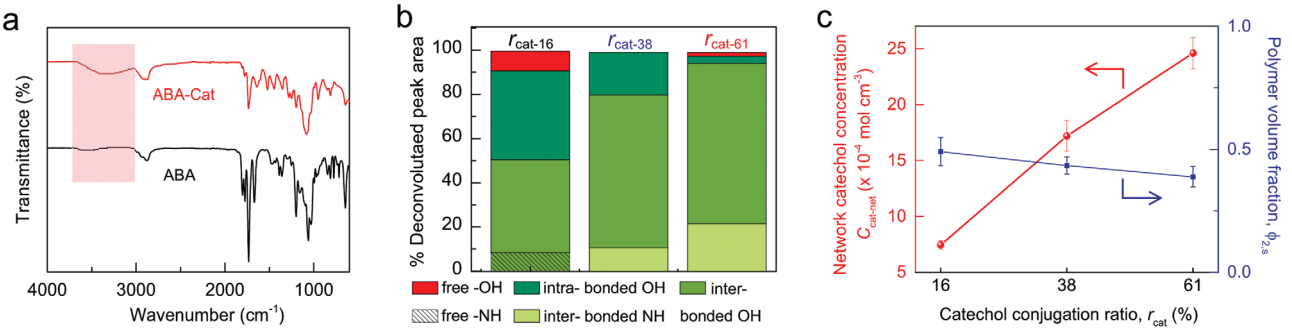


**Figure 1.** a) FTIR spectra of crosslinked networks composed of ABA and ABA-Cat precursor polymers. The characteristic peak in the shaded region indicates hydrogen bonding in ABA-Cat networks. b) Normalized areas after peak deconvolution between 3700 and 3100 $cm^{-1}$ for $r_{cat\text{-}16}$, $r_{cat\text{-}38}$, and $r_{cat\text{-}61}$. c) Catechol conjugation ratio ($r_{cat}$) dependence of the network catechol concentration ($C_{cat\text{-}net}$) and the polymer volume fraction of the swollen network ($\phi_{2,s}$).

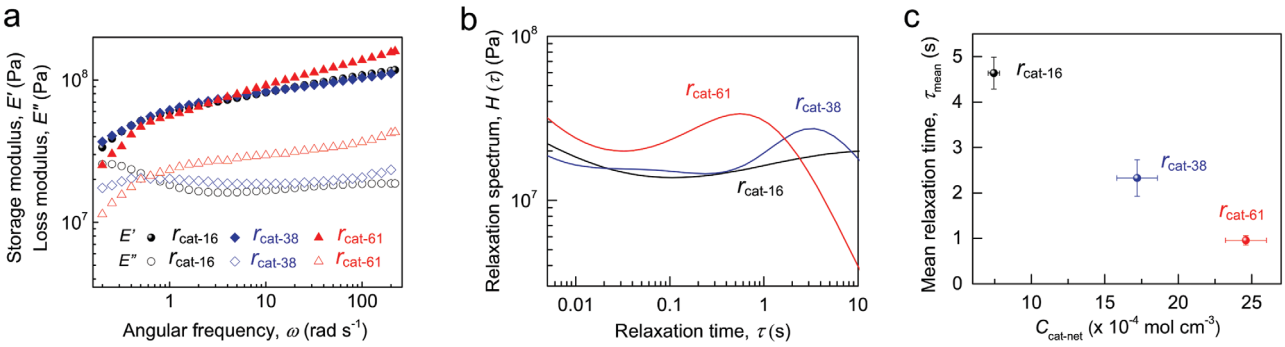


**Figure 2.** The effect of the network catechol concentration on the network dynamic mechanical properties. a) The storage $E'$ and loss moduli $E''$ of networks prepared from $r_{cat\text{-}16}$, $r_{cat\text{-}38}$, and $r_{cat\text{-}61}$ polymers are plotted as a function of angular frequency obtained from tensile oscillatory sweeps ($\varepsilon = 0.1\%$; $\omega = 0.2$ to 220 rad s$^{-1}$). b) Calculated relaxation time spectra of the $r_{cat\text{-}16}$, $r_{cat\text{-}38}$, and $r_{cat\text{-}61}$ networks, showing two distinct features. The spectra calculated from both $E'$ and $E''$ data (see detailed methods in Supporting Information). c) Dependence of mean relaxation time of reversible bond derived from the relaxation spectra.

The viscoelastic properties of ABA-Cat networks are a strong function of $C_{cat\text{-}net}$ (**Figure 2**). Networks prepared from $r_{cat\text{-}16}$, $r_{cat\text{-}38}$, and $r_{cat\text{-}61}$ precursor polymers exhibit solid-like behavior with $E' \approx 20$–30 MPa, values that increase monotonically as $\omega$ increases from 0.2 to 200 rad s$^{-1}$. The loss modulus is a strong function of catechol concentration. In networks prepared from $r_{cat\text{-}16}$ polymers, the trend in $E''$ versus $\omega$ exhibits two rounded features in the range of $\omega = 0.2$ to 2 rad s$^{-1}$ and $\omega = 2$ to 220 rad s$^{-1}$, respectively. As $r_{cat}$ increases, the rounded peaks shift toward higher frequencies, as shown in Figure 2a for the networks prepared from polymers with $r_{cat\text{-}38}$ and $r_{cat\text{-}61}$. Networks prepared from $r_{cat\text{-}61}$ polymers have a very board feature that spans the entire frequency range tested in this study. These data suggest that the relaxation time distribution broadens as $C_{cat\text{-}net}$ increases.[30,31] The two features in loss modulus suggest two relaxation modes are present: crosslink scission and chain motion.[32,33] Rouse type chain motion typically produces features at high frequencies as predicted by sticky-repetition theory and observed in previous studies.[34,35] The quick motion feature is assigned to the Rouse motion of PEG-based B blocks. The low glass transition temperature ($T_{g\text{-}PEG} = -60$ °C) and hygroscopic nature of PEG suggest B blocks in hydrated networks are highly mobile at room temperature. The feature associated with comparatively long relaxation times is attributed to the reversible bond cleavage and formation.[33] The time scale associated with the frequency spectrum (Figure 2b) most prominent part of this feature is comparable to that of hydrogen bonded networks in previous studies with $\tau \approx 0.1$ to 6 s.[26,36,37]

The mean bond lifetime of reversible junctions can be extrapolated from the relaxation spectrum using a method adapted from Grindy et al.,[23] which assumes the components can each be described by Maxwell behavior. The two features of loss modulus suggest two-mode log-normal distribution of relaxation time. The spectra (Figure 2b) are calculated from experimentally determined values of $E'(\omega)$ and $E''(\omega)$. The fitted storage modulus and loss modulus can then be determined by integrating the relaxation spectrum. The calculated modulus is in good agreement with experimentally determined values (Figure S3, Supporting Information), which suggests the methodology is accurate. The mean relaxation time obtained for the junctions in the network is inversely related with $C_{cat\text{-}net}$ (Figure 2c). This result appears to contradict trends predicted from reversible network theories, which assert that the characteristic relaxation times increase exponentially with the density of motifs.[38,39] This model predicts terminal relaxation time of the network wherein increasing the concentration of interacting motifs retards whole chain motion, a phenomenon that is difficult to observe in frequencies measured in this study. Conversely, the concept of renormalized bond lifetime proposed by Rubinstein et al.[40,41] can better explain our experimental observations. This idea suggests after the unbinding of a reversible junction, self-recombination cannot relax the stressed chain until the dislocated bond reforms with another available neighbor. Self-recombination can thus increase the characteristic time scale for relaxation. The effective concentration of catechols in the physical crosslinks rich in A blocks increases proportionally with $r_{cat}$ (Figure 1c). The characteristic length scale between pendant catechols is inversely related to $C_{cat\text{-}net}$. As such, the probability that nascently ruptured catechol motifs reform is proportional to $C_{cat\text{-}net}$.

The time scale for recovery of intermolecular bonding within physical crosslinks is also inversely proportional to the concentration of catechols as the network is macroscopically deformed under uniaxial strain (**Figure 3**). The toughness ($U_T$) and extensibility ($\varepsilon_{max}$) of networks increase with $C_{cat\text{-}net}$. Values for $U_T$ and $\varepsilon_{max}$ increase from 0.15 ± 0.05 to 1.51 ± 0.06 J m$^{-3}$ and from 0.14 ± 0.04 to 1.33 ± 0.07 mm mm$^{-1}$, respectively, as the $r_{cat}$ of ABA triblocks increases (Figure 3a; Table S3, Supporting Information). The increase of toughness is consistent with Lake–Thomas theory $W = \sum U$ ($\sum$ is density of reconfigurable bonds, bonds nm$^{-3}$; $U$ is the energy needed to break a reconfigurable bond). Cyclic recovery tests (Figure 3b and Figure S4, Supporting Information) were performed on networks prepared from polymers composed of $r_{cat\text{-}16}$, $r_{cat\text{-}38}$, and $r_{cat\text{-}61}$ ABA-Cat. Reforming reconfigurable bonds can be indirectly measured by comparing the tensile work under sequential loading, defined by $W_{load\text{-}2nd}/W_{load\text{-}1st} \times 100\%$, to obtain resilience recovery ratio ($R_t$) at recovery time $t$ s.[6,11] All networks can achieve $R_t$ of 100%, given sufficient recovery time (Figure 3c). Mechanical responses of the networks for large deformation show the same trend with that for small deformation from DMA analysis. At large deformation, the strain

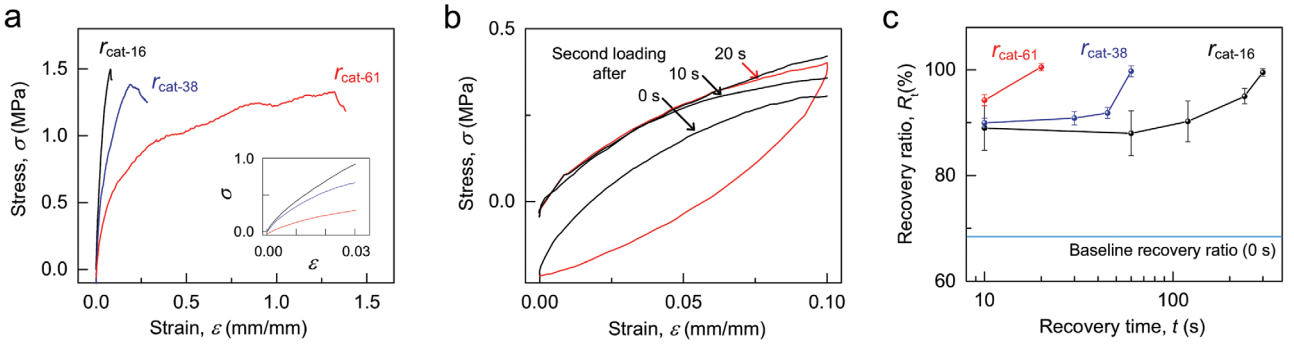


**Figure 3.** The effect of the network catechol concentration on the mechanical response of networks under unaxial strain. a) Tensile behavior of the ABA-Cat networks prepared from polymers with varying $r_{cat}$. b) Cyclic loading of the network of $r_{cat-61}$ from the first cycle with specified dwell time as labeled (see Figure S4, Supporting Information for $r_{cat-16}$ and $r_{cat-38}$ samples). c) Relationship between recovery time and recovery ratio in networks of prescribed composition where the recovery ratio is defined as the ratio of (tensile work of cycle $n = 2$):(tensile work of cycle $n = 1$). These results suggest that networks prepared from polymers with larger values of $r_{cat}$ can recover from mechanical strains more rapidly and thus restore network elasticity more efficiently when compared to networks prepared from polymers with smaller values of $r_{cat}$.

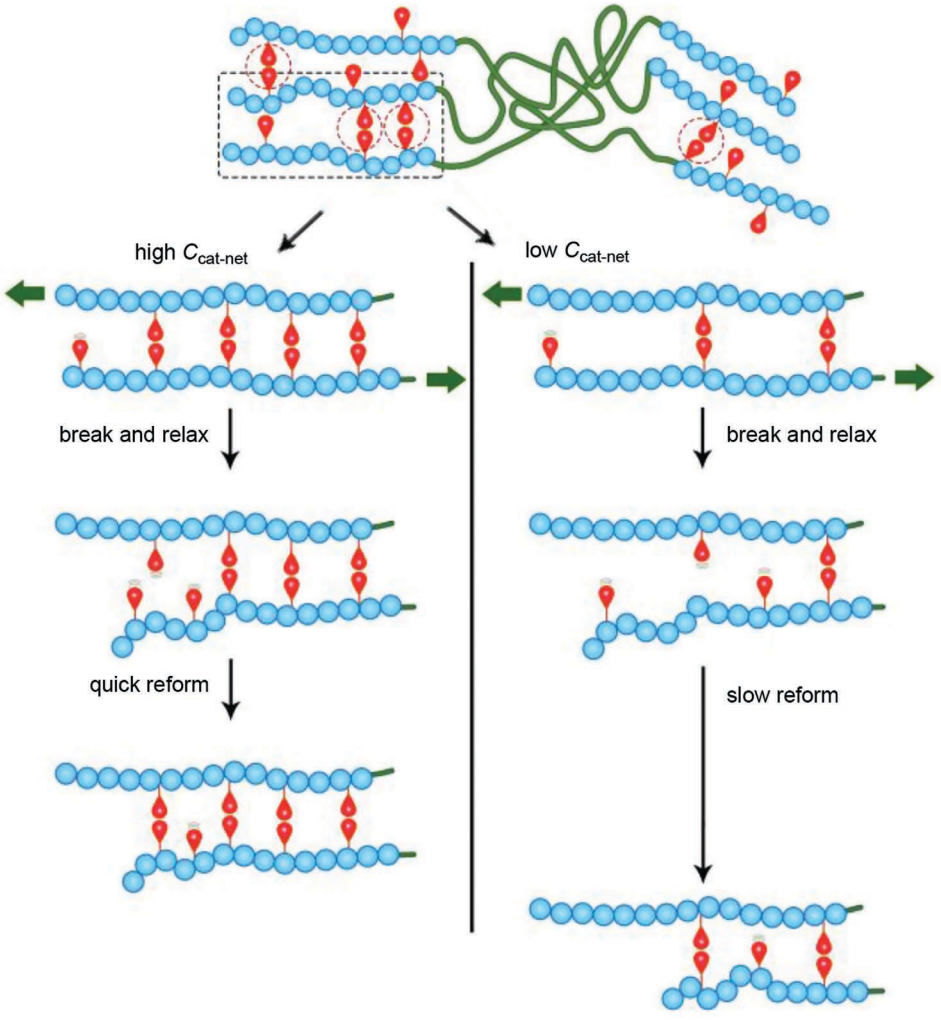


**Figure 4.** Proposed molecular model to describe trends in time scale for reversible bonds versus $C_{cat-net}$ in ABA-Cat networks under mechanical loading. First row is the initial state of reversible junctions. After stretching the network, the junctions break, and the chains relax. Dislocated bonds reform with nearby available motifs at a rate that depends on $C_{cat-net}$. Networks with relatively higher concentrations lead to quick reformation while those with smaller concentrations of catechols exhibit slow reformation.

energy carried by a stretched polymer chain can be released when it detaches from a junction as shown in **Figure 4**.[42–44] When the breaking bond finds a new partner near it, it can recombine and contribute to the network stress and modulus from a new relaxed conformation. The recombination time is therefore dependent on the concentration of motifs that can create reconfigurable bonds.

Catechol-bearing PEG-based ABA triblock polymers self-assemble into mechanically robust networks with hydrogen bonded physical crosslinks enriched in A blocks. The resulting networks are mechanically robust ($E$ = 16.2 ± 2.5 MPa), extensible ($\varepsilon_{max}$ = 1.33 ± 0.07 mm mm$^{-1}$), and tough (≈1.5 ± 0.06 MJ m$^{-3}$). The concentration of inter- and intramolecular bonding within physical crosslinks determines the dominant relaxation modes and, ultimately, the characteristic time scale to recover from large uniaxial tensile strains. Furthermore, experimentally observed trends in relaxation time scales for hydrogen bonded networks described here are consistent with previously established theories. Based on these findings, it may be possible to control the time scale for network relaxation by exploiting other types of reconfigurable bonds including multivalent ion bridges or coordination bonds. Doing so could further enhance the dissipative modes and potentially enhance prospective macroscopic properties such as toughness or interfacial adhesion. The molecular topology could also be expanded and refined including, potentially, the investigation for structure–property relationships in ABC triblock copolymers[45] or star-shaped polymers including Miktoarm polymers. Enhancing the performance of this class of polymers could further expand the use of this material in consumer products, marine applications, or surgical materials.

## Supporting Information

Supporting Information is available from the Wiley Online Library or from the author.

## Acknowledgements

X.-M.T. thanks the following people for the help and discussion of synthesis and mechanical characterization: Xitong Liu, Pengpeng, and Bill Pingitore. The authors acknowledge the financial support provided by the following organizations: National Institutes of Health (R21NS095250); the Defense Advanced Research Projects Agency (D14AP00040); the National Science Fundation (DMR1542196). The authors would also like to thank the CMU Thermomechanical Characterization Facility in the Department of Materials Science and Engineering and NMR instrumentation at Carnegie Mellon University (CHE-0130903, CHE-1039870, and CHE-1726525).

## Conflict of Interest

The authors declare no conflict of interest.

## Keywords

catechol, hydrogen bond network, self-assembly, self-healing

Received: October 15, 2019
Revised: November 13, 2019
Published online: December 26, 2019

[1] J. P. Gong, Y. Katsuyama, T. Kurokawa, Y. Osada, *Adv. Mater.* **2003**, *15*, 1155.
[2] C . Creton, *Macromolecules* **2017**, *50*, 8297.
[3] T. L. Sun, T. Kurokawa, S. Kuroda, A. B. Ihsan, T. Akasaki, K. Sato, M. A. Haque, T. Nakajima, J. P. Gong, *Nat. Mater.* **2013**, *12*, 932.
[4] Y. N. Ye, M. Frauenlob, L. Wang, M. Tsuda, T. L. Sun, K. P. Cui, R. Takahashi, H. J. Zhang, T. Nakajima, T. Nonoyama, T. Kurokawa, S. Tanaka, J. P. Gong, *Adv. Funct. Mater.* **2018**, *28*, 1801489.
[5] P. Cordier, F. Tournilhac, C. Soulie-Ziakovic, L. Leibler, *Nature* **2008**, *451*, 977.
[6] Q. H. Zhang, X. Y. Zhu, C. H. Li, Y. F. Cai, X. D. Jia, Z. N. Bao, *Macromolecules* **2019**, *52*, 660.
[7] C. H. Li, C. Wang, C. Keplinger, J. L. Zuo, L. Jin, Y. Sun, P. Zheng, Y. Cao, F. Lissel, C. Linder, X. Z. You, Z. A. Bao, *Nat. Chem.* **2016**, *8*, 619.
[8] J. Y. Sun, X. H. Zhao, W. R. K. Illeperuma, O. Chaudhuri, K. H. Oh, D. J. Mooney, J. J. Vlassak, Z. G. Suo, *Nature* **2012**, *489*, 133.
[9] Z. Lv, J. N. Qiao, Y. N. Song, X. Ji, J. H. Tang, D. X. Yan, J. Lei, Z. M. Li, *ACS Appl. Mater. Interfaces* **2019**, *11*, 12008.
[10] J. A. Neal, D. Mozhdehi, Z. B. Guan, *J. Am. Chem. Soc.* **2015**, *137*, 4846.
[11] M. Y. Guo, L. M. Pitet, H. M. Wyss, M. Vos, P. Y. W. Dankers, E. W. Meijer, *J. Am. Chem. Soc.* **2014**, *136*, 6969.
[12] S. H. Hong, S. Kim, J. P. Park, M. Shin, K. Kim, J. H. Ryu, H. Lee, *Biomacromolecules* **2018**, *19*, 2053.
[13] H. J. Zhang, T. L. Sun, A. K. Zhang, Y. Ikura, T. Nakajima, T. Nonoyama, T. Kurokawa, O. Ito, H. Ishitobi, J. P. Gong, *Adv. Mater.* **2016**, *28*, 4884.
[14] P. G. Khalatur, A. R. Khokhlov, D. A. Mologin, *J. Chem. Phys.* **1998**, *109*, 9602.
[15] Z. P. Xu, *Sci. Rep.* **2013**, *3*, 2914.
[16] N. Holten-Andersen, M. J. Harrington, H. Birkedal, B. P. Lee, P. B. Messersmith, K. Y. C. Lee, J. H. Waite, *Proc. Natl. Acad. Sci. USA* **2011**, *108*, 2651.
[17] S. B. Xu, D. K. Sheng, X. D. Liu, F. C. Ji, Y. Zhou, L. Dong, H. H. Wu, Y. M. Yang, *Polym. Int.* **2019**, *68*, 1084.
[18] Y. Liu, H. Meng, Z. Qian, N. Fan, W. Choi, F. Zhao, B. P. Lee, *Angew. Chem., Int. Ed.* **2017**, *56*, 4224.
[19] E. Filippidi, T. R. Cristiani, C. D. Eisenbach, J. H. Waite, J. N. Israelachvili, B. K. Ahn, M. T. Valentine, *Science* **2017**, *358*, 502.
[20] M. K. Włodarczyk-Biegun, J. I. Paez, M. Villiou, J. Feng, A. Del Campo, bioRxiv 599290, **2019**.
[21] S. C. Grindy, M. Lenz, N. Holten-Andersen, *Macromolecules* **2016**, *49*, 8306.
[22] N. Holten-Andersen, A. Jaishankar, M. J. Harrington, D. E. Fullenkamp, G. DiMarco, L. H. He, G. H. McKinley, P. B. Messersmith, K. Y. C. Lee, *J. Mater. Chem. B* **2014**, *2*, 2467.
[23] S. C. Grindy, R. Learsch, D. Mozhdehi, J. Cheng, D. G. Barrett, Z. B. Guan, P. B. Messersmith, N. Holten-Andersen, *Nat. Mater.* **2015**, *14*, 1210.
[24] V. Barone, I. Cacelli, A. Ferretti, G. Prampolini, *Biomimetics* **2017**, *2*, 18.
[25] L. Li, B. Yan, J. Q. Yang, L. Y. Chen, H. B. Zeng, *Adv. Mater.* **2015**, *27*, 1294.
[26] X. M. Tang, C. J. Bettinger, *J. Mater. Chem. B* **2018**, *6*, 545.
[27] W. Wei, L. Petrone, Y. P. Tan, H. Cai, J. N. Israelachvili, A. Miserez, J. H. Waite, *Adv. Funct. Mater.* **2016**, *26*, 3496.
[28] S. H. M. Sontjens, R. A. E. Renken, G. M. L. van Gemert, T. A. P. Engels, A. W. Bosman, H. M. Janssen, L. E. Govaert, F. P. T. Baaijens, *Macromolecules* **2008**, *41*, 5703.

 

[29] A. N. Semenov, J. F. Joanny, A. R. Khokhlov, *Macromolecules* **1995**, *28*, 1066.
[30] L. L. D. Freitas, R. Stadler, *Macromolecules* **1987**, *20*, 2478.
[31] R. Stadler, L. D. Freitas, *Colloid Polym. Sci.* **1986**, *264*, 773.
[32] B. L. Smith, T. E. Schaffer, M. Viani, J. B. Thompson, N. A. Frederick, J. Kindt, A. Belcher, G. D. Stucky, D. E. Morse, P. K. Hansma, *Nature* **1999**, *399*, 761.
[33] L. Leibler, M. Rubinstein, R. H. Colby, *Macromolecules* **1991**, *24*, 4701.
[34] K. Y. Xing, M. Tress, P. F. Cao, F. Fan, S. W. Cheng, T. Saito, A. P. Sokolov, *Macromolecules* **2018**, *51*, 8561.
[35] F. Tanaka, S. F. Edwards, *Macromolecules* **1992**, *25*, 1516.
[36] X. B. Hu, J. Zhou, W. F. M. Daniel, M. Vatankhah-Varnoosfaderani, A. V. Dobrynin, S. S. Sheiko, *Macromolecules* **2017**, *50*, 652.
[37] M. Wubbenhorst, J. van Turnhout, B. J. B. Folmer, R. P. Sijbesma, E. W. Meijer, *IEEE Trans. Dielectr. Electr. Insul.* **2001**, *8*, 365.
[38] R. J. J. Jongschaap, R. H. W. Wientjes, M. H. G. Duits, J. Mellema, *Macromolecules* **2001**, *34*, 1031.
[39] M. Rubinstein, A. N. Semenov, *Macromolecules* **1998**, *31*, 1386.
[40] I. A. Nyrkova, A. N. Semenov, *Europhys. Lett.* **2007**, *79*, 66007.
[41] M. Rubinstein, A. N. Semenov, *Macromolecules* **2001**, *34*, 1058.
[42] R. Long, K. Mayumi, C. Creton, T. Narita, C. Y. Hui, *Macromolecules* **2014**, *47*, 7243.
[43] J. Liu, C. S. Y. Tan, Z.-Y. Yu, Y. Lan, C. Abell, O. A. Scherman, *Adv. Mater.* **2017**, *29*, 1604951.
[44] J. Y. Guo, R. Long, K. Mayumi, C. Y. Hui, *Macromolecules* **2016**, *49*, 4378.
[45] J. Qin, F. S. Bates, D. C. Morse, *Macromolecules* **2010**, *43*, 5128.